Abdominal Radiology (2019) 44:2594–2601
https://doi.org/10.1007/s00261-019-01982-9

INTERVENTIONAL RADIOLOGY

Using principal component analysis for the prediction of tumor response to transarterial chemoembolization

Jessica P. Miller[1] · **Raja Ramaswamy**[2] · **Olaguoke Akinwande**[2]

Published online: 19 April 2019

Abstract

Purpose To quantitate the tumor blush of hepatocellular carcinoma (HCC) at the time of transarterial chemoembolization (TACE) using principal component analysis (PCA), and to correlate the quantitated tumor blush to response to therapy.

Materials and methods In this proof-of-concept study, 27 primary HCC tumors in 25 patients (18 men, 7 women; mean age 66 years ± 9) were analyzed. We conducted a retrospective analysis of TACE procedures that were performed during March through July of 2017. Digital subtraction angiography (DSA) was combined with PCA to condense spatial and temporal information into a single image. The tumor and liver contrast enhancements were calculated, and the ratio was used to determine the relative vascular enhancement of the tumor. Tumor response to therapy was determined at 1-month post procedure.

Results Using PCA-generated fluoroscopic imaging (PCA-FI), we quantitated the tumor blush and assigned a vascular enhancement value (VEV) to each tumor. Tumors that responded to treatment ($N = 12$) had statistically higher VEVs compared with the nonresponders ($N = 15$), with a mean value of 0.96 ± 0.455 vs. 0.57 ± 0.309, ($p = 0.013$).

Conclusions We developed a method for quantitating tumor blush using routine angiographic images. The VEVs calculated using these images may allow for the prediction of tumor response to therapy. This pilot study suggests that there is a correlation between tumor blush intensity and tumor response.

Keywords Fluoroscopy · Angiogram · Quantitative · Perfusion · TACE · Hepatocellular carcinoma

Introduction

Hepatocellular carcinoma (HCC) is the most common primary hepatic malignancy and is the fifth most common cancer in men, and the seventh most common cancer in women worldwide [1]. Transarterial chemoembolization (TACE) is routinely used to treat HCC [2–4]. Currently, the tumor response to TACE therapy is unknown until the postprocedure follow-up imaging, typically conducted via cross-sectional imaging at one month post-TACE. Researchers have sought to discover a means to predict tumor response at the point-of-care to determine adequacy of treatment. This may allow for patient-specific tailoring of postprocedural surveillance and for managing patient expectations.

Prior studies have demonstrated that tumor arterial perfusion is linked to deposition of embolic material and response to TACE [5, 6]. We hypothesize that the quantitated degree of tumor blush during TACE may be indicative of tumor response to therapy. To investigate this, we developed a standardized method for capturing the overall tumor perfusion from angiograms obtained during TACE. This method combines tumor perfusion and principal component analysis (PCA) to both visualize tumors and predict the tumor response to TACE at the point-of-care.

Materials and methods

Patients

This study was a retrospective single-center analysis of patients with HCC who underwent TACE to determine if images from TACE could predict tumor response.

✉ Jessica P. Miller
miller.jessica@wustl.edu

[1] Washington University School of Medicine, 660 S. Euclid Ave., St. Louis, MO 63110, USA

[2] Department of Interventional Radiology, Washington University School of Medicine, 510 S. Kingshighway Blvd, St. Louis, MO 63110, USA

Institutional Review Board (IRB) approval was obtained prior to this study, and all data analysis followed HIPAA compliance. Informed consent was waived for this retrospective study. TACE procedures from March 2017 through July 2017 were included in our analysis. Our initial search returned 40 procedures. Procedures were excluded if there was no follow-up imaging in our system within 3 months ($N = 5$), there was no angiogram recorded in the patient medical record or the angiogram was of insufficient length to delineate the vasculature ($N = 7$), or there was significant imaging artifact produced during the angiogram ($N = 1$). Each tumor analyzed was treated as a separate event. Our final study group consisted of 27 primary HCC tumors in 25 patients. The mean patient age was 66 y ± 9 (18 men, 7 women). Baseline patient demographics and tumor characteristics were captured from chart review and are shown in Table 1.

Table 1 Patient baseline demographics and tumor characteristics

Demographics	Values
Total number of patients	25
Total number of tumors	27
Age	66 ± 9
Gender	
Male	18 (72%)
Female	7 (28%)
Primary HCC	25 (100%)
Background disease process	
Cirrhosis	15 (60%)
NASH	2 (8%)
Hep C (without cirrhosis)	4 (16%)
Unknown	4 (16%)
Prior number of embolization procedures	
Mean	1.07 ± 1.62
Median (range)	0 (0–6)
Receiving systemic chemotherapy	1 (8%)
Length of target tumor (cm)	4.3 ± 3.21
Liver segment involved	
Segment I	0 (0%)
Segment II	3 (11%)
Segment III	0 (0%)
Segment IV	4 (15%)
Segment V	7 (26%)
Segment VI	6 (22%)
Segment VII	5 (19%)
Segment VIII	2 (7%)

Percentages were calculated based on the total number of primary tumors

TACE procedure

All patients received doxorubicin chemoembolization in the procedure under analysis. Hepatic angiography was performed in standard fashion. In brief, through femoral arterial access, the celiac artery was selected. Next, the hepatic artery was selected using the base 5F catheter or a microcatheter. A hepatic angiogram was performed to delineate the anatomy with delayed images to identify areas of abnormal vascular perfusion (tumor blush). The DSA delineated the tissue that was well perfused by the contrast media injection, including both the tumor vasculature and the feeding artery. The time series of images contained within the DSA file were used to create a reproducible and quantifiable method to assess tumor perfusion dynamics during TACE.

Quantitative image analysis

We developed a method to visualize the time-behavior of the tumor vasculature in a single image such that we could analyze it further. To accomplish this, we utilized PCA and a custom-developed image-processing algorithm to enhance flexibility in image analysis. In using PCA to identify the vasculature, we were able to capture the spatiotemporal behavior of the angiogram in a single image [7]. Because our method was executed using nonproprietary code, we were able to conduct further post processing to understand the behavior of the system. We termed this approach PCA-generated fluoroscopic imaging (PCA-FI).

Angiograms were obtained using standard procedural techniques and then analyzed post hoc. By doing so, we ensured that our analysis was compatible with the procedural workflow. Angiograms were 1024 × 1024 pixels and consisted of a minimum of five frames. They were imported into MATLAB (Mathworks, Inc., Natick, MA) as a time-series of images and analyzed via the "pca" command (Fig. 1a). PCA allows for reducing multidimensional datasets into a lower number of dimensions, while continuing to describe the behavior of the dataset [7]. The components that describe the system are termed principal components (PCs) and are numbered in order of significance, so variables that do not characterize the system are minimized (Fig. 1b). Angiograms obtained within the workflow of a procedure are inherently variable due to catheter positioning, contrast bolus volume, length of the imaging run, patient motion, and other variables. PCA minimizes sources of variability which was advantageous for angiogram analysis.

Using a single representative angiogram, a PCA-FI image representing the first four PCs was generated

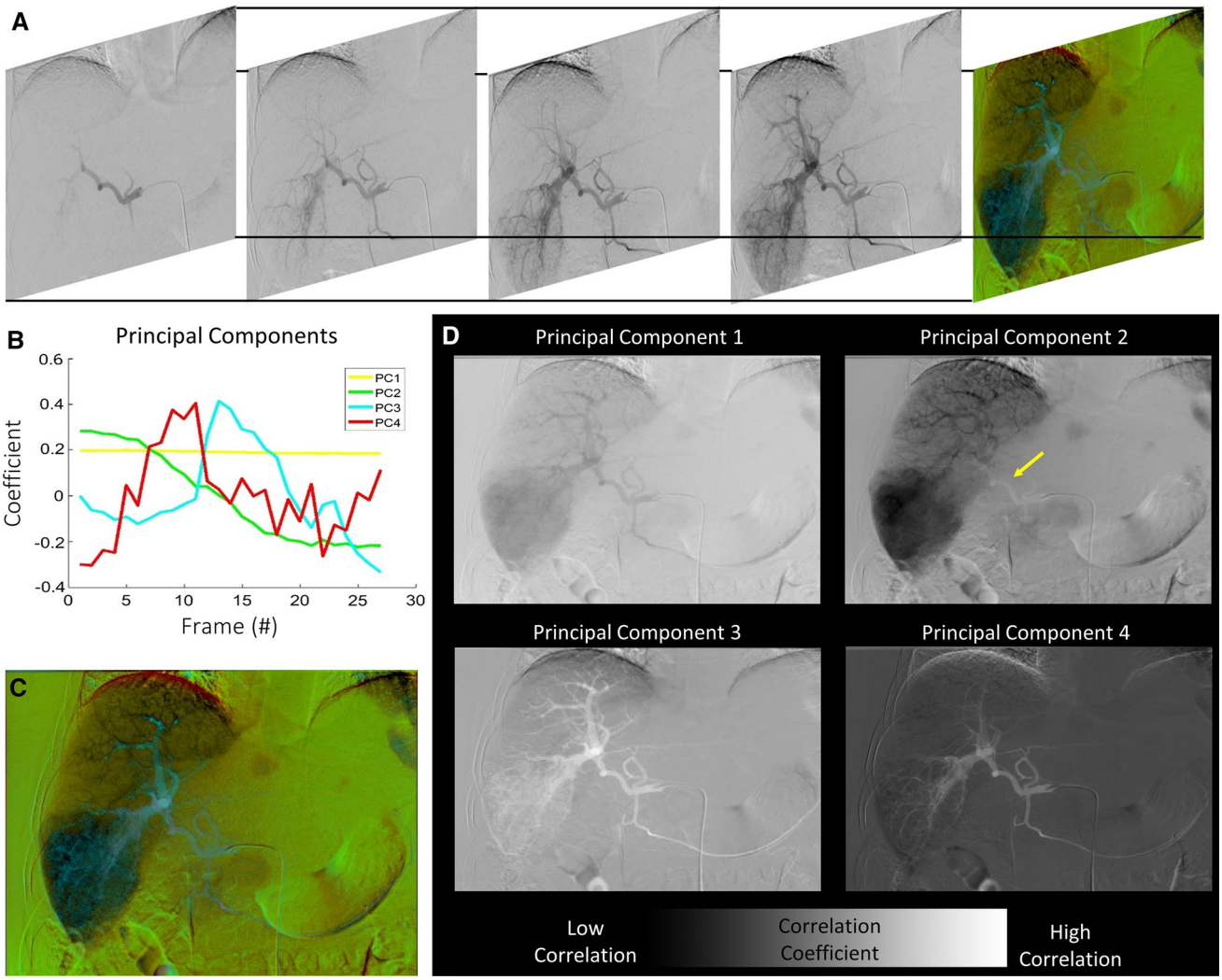

Fig. 1 **a** Representative successive angiographic images throughout a contrast bolus injection into the hepatic artery. Final image on right is the color representation of the principal components (PCs) spatially distributed (PCA-FI image). **b** PC coefficients over time (frame #) for the first four PCs, with colors corresponding to the PCA-FI image. **c** Representative PCA-FI image. Each color representing a different PC, and each pixel's color opacity weighted by the PC correlation coefficient. **d** Each PC displayed individually in grayscale. Regions of high correlation to the PC represented with white and low correlation with black (opposite of DSA images). PC1 was highly correlated to regions that were not enhanced by contrast. PC2 was correlated with contrast in the proper hepatic artery (yellow arrow). PC3 and PC4 correlated with contrast in the vascular tree. Note the scales vary between images as they are normalized by the max and min coefficients (which vary between each PC)

(Fig. 1c). We investigated including additional PCs; however, PCs greater than 4 produced regions that did not have a physical correlate. Using PCs 1–4, the PC correlation coefficient was computed for each pixel in the image stack, and each pixel was assigned a color that corresponded to the PC. Pixels that corresponded with a particular PC were assigned the same color throughout the image, and the opacity of that color was determined by the magnitude of the correlation coefficient [7–10]. An increased opacity corresponded to a higher correlation coefficient, and negative correlations were set to translucent. In the case where multiple PCs had a positive correlation coefficient within the same pixel, the hue of the pixel was rendered using a mixture of colors.

PCA-FI tumor identification

PCA-FI was used to generate images that represented the spatiotemporal behavior of the contrast media within the tumor. In the PCA-FI images, a pixel rendered with increased opacity corresponded to a higher correlation to the contrast media injection behavior over time. The hue of each pixel was a mixture of colors depending on the principal components that had a positive correlation with that

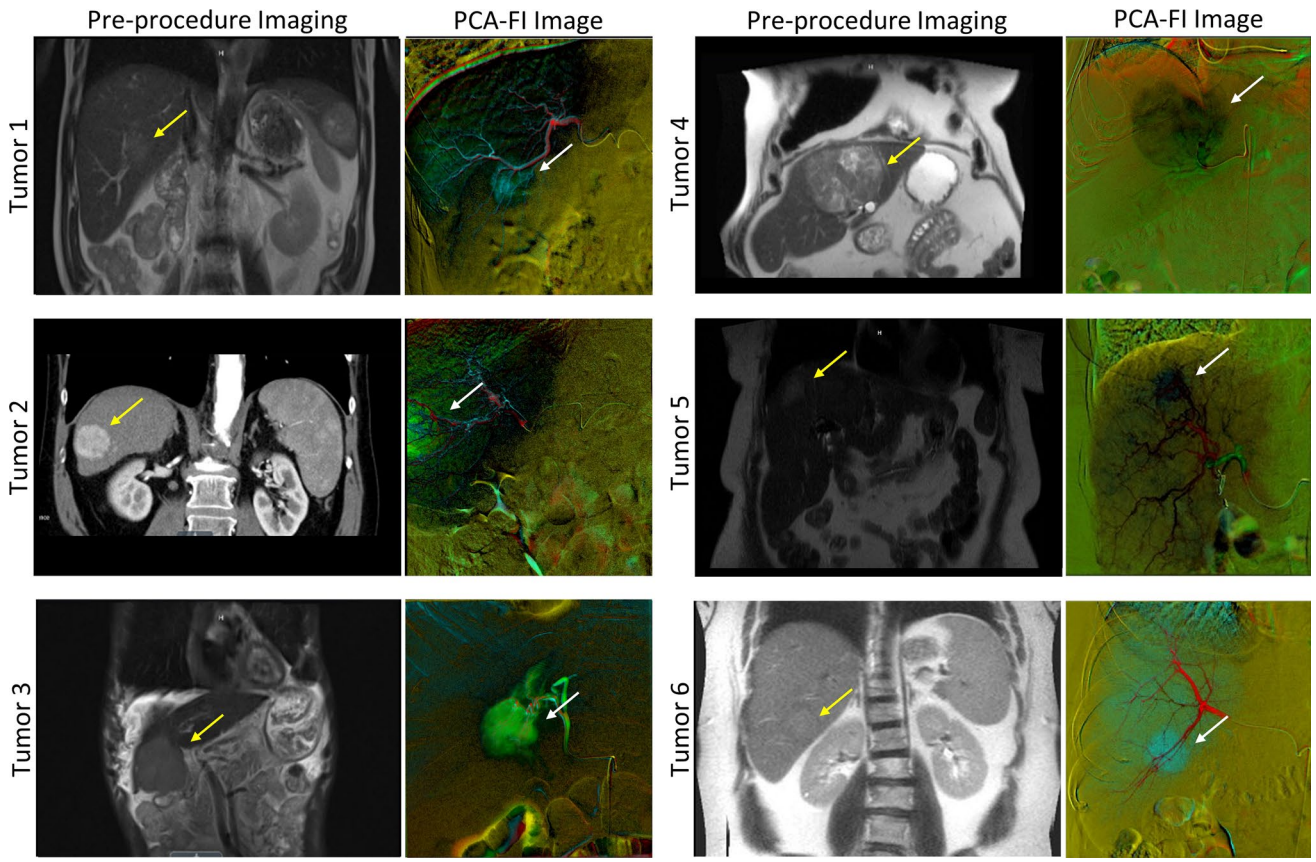

Fig. 2 Representative CT or MR preprocedure images on the left, and PCA-FI images on the right. Tumor locations indicated by a yellow arrow for the CT and MR images, and white arrow for the PCA-FI images; both showing spatial agreement

pixel. We compared the PCA-FI images to the preprocedure MR and CT images, and confirmed that the algorithm was correctly identifying tumors (Fig. 2).

Quantitative tumor vascular enhancement

We then sought to quantitate our images in a manner that would allow for comparison of tumor enhancement across imaging runs. Grayscale principal component maps were generated that consisted of the sum of the PCA correlation coefficients for each pixel with the background component removed (Fig. 3a). In summing the correlation coefficients, pixels with a high degree of vascular involvement were weighted more heavily than pixels outside of the target vasculature.

The principal component maps provided a spatial understanding of the pixels that behaved similarly throughout the bolus injection; however, they did not fully explain the contrast media dwell behavior. Regions of interest (ROIs) were generated to isolate the structures of interest for further analysis (Fig. 3b, c). To quantitate the pooling of the contrast bolus, we calculated the intensity area under the curve (AUC) for each pixel within the ROIs (Fig. 3d). The AUC was calculated by taking the integral of the contrast intensity over the time of the injection (Eq. 1), and was greater for the tumors compared to the surrounding liver parenchyma (Fig. 3e). The contrast media pooling was linked to the vascular map by multiplying the AUC by the principal component map in a pixel-wise fashion (Eq. 2).

$$[\mathrm{AUC}]_{x,y} = \int_0^t [\mathrm{CI}(\tau)]_{x,y} \mathrm{d}\tau \tag{1}$$

$$[\mathrm{VE_{map}}]_{x\cdot y} = \left[\mathrm{PC_{map}}\right]_{x\cdot y} \cdot [\mathrm{AUC}]_{x\cdot y}, \tag{2}$$

where CI is the contrast intensity of each bolus injection, τ is the integration constant, and t is the time of the bolus injection. $\mathrm{VE_{map}}$ is the vascular enhancement map calculated by pixel-wise multiplication.

We created a vascular enhancement value (VEV) by dividing the tumor-to-liver AUC by the pretreatment tumor length. The VEV (normalized tumor blush) captured the

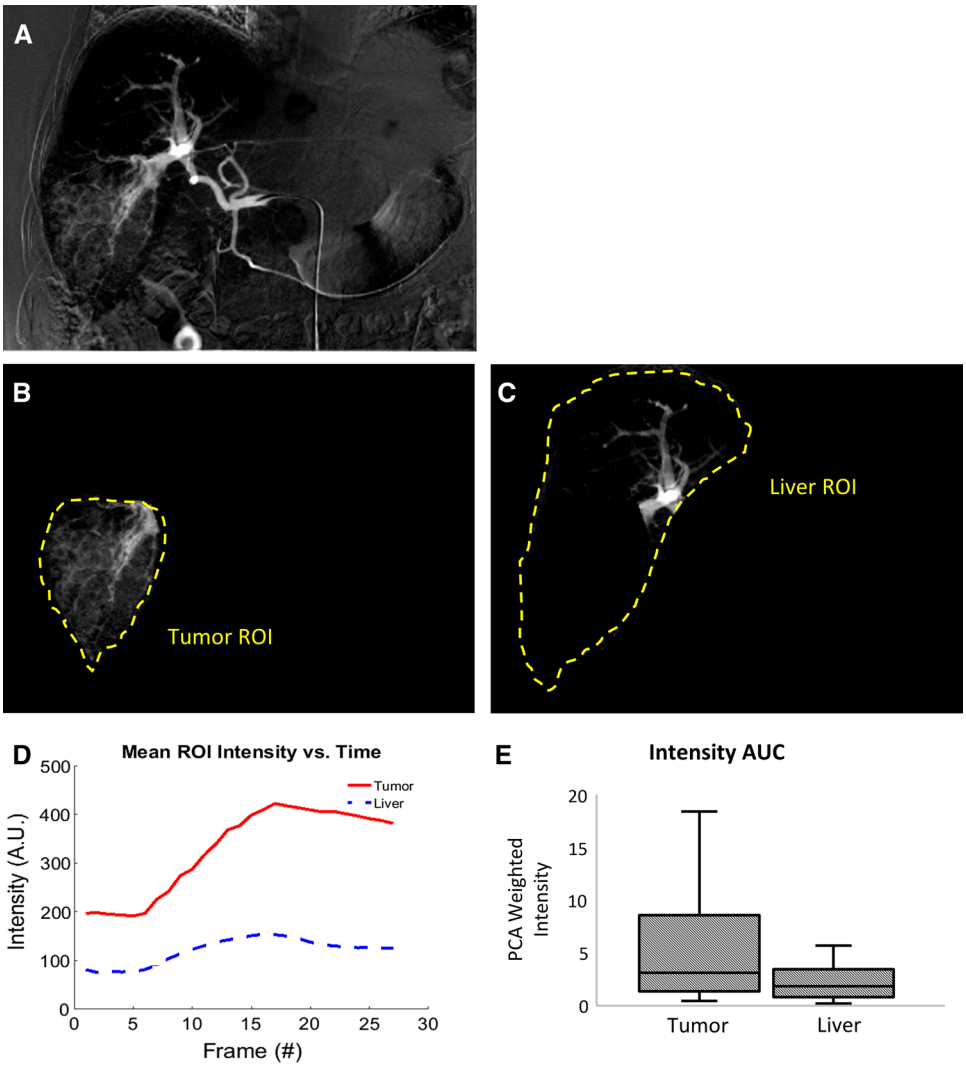

Fig. 3 **a** Principal component map containing PC2, PC3, and PC4, with PC1 removed as the background signal. **b** Tumor ROI outlined, and **c** Liver ROI outlined. Contained tumor ROI removed from Liver ROI. **d** Representation of the mean contrast intensities for the tumor (solid line) and liver (dashed line) ROIs throughout the bolus of injected contrast media. The AUC for each pixel was calculated and used as a weighting factor in creating the vascular enhancement value. **e** Mean intensity AUC for the tumor and liver for each angiogram

relative tumor perfusion in a reproducible manner. Equations 3–5 show the calculation of the VEV.

$$\mathrm{AUC}_{\mathrm{tumor}} = \frac{1}{n}\sum_{i=1}^{n}\left[\mathrm{VE}_{\mathrm{map}}(i)\right]_{xt,yt} \tag{3}$$

$$\mathrm{AUC}_{\mathrm{liver}} = \frac{1}{m}\sum_{i=1}^{m}\left[\mathrm{VE}_{\mathrm{map}}(i)\right]_{xl,yl} \tag{4}$$

$$\mathrm{VEV} = \frac{\mathrm{tumor}}{\mathrm{liver}} \div \mathrm{length}, \tag{5}$$

where $\mathrm{AUC}_{\mathrm{tumor}}$ and $\mathrm{AUC}_{\mathrm{liver}}$ represent the tumor and liver signals, respectively. The pixels within the tumor and liver ROIs are represented by *xt*,*yt*, and *xl*,*yl*, respectively. *n* and *m* represent the number of pixels within each ROI. The tumor length was the longest dimension (estimated linear diameter), reported by the preprocedural MR or CT imaging.

Statistical analysis

Tumor response to therapy was determined using the follow-up CT or MR image at 1-month post procedure. One patient received additional therapy to a separate vascular supply, so the follow-up imaging was delayed to 3-months post procedure. The modified Response Evaluation Criteria in Solid Tumors (mRECIST) was used to classify clinical tumor response [11]. The mRECIST criteria were converted into a numeric scale with a complete response (CR) = 4, partial response (PR) = 3, stable disease (SD) = 2, and progressive disease (PD) = 1. Data were analyzed using PRISM

(GraphPad Software, Inc., La Jolla, CA). The difference between means was analyzed using an unpaired, two-tailed *t* test, with $p < 0.05$ considered significant. Correlation was tested using the Pearson correlation coefficient. Multivariate analysis was conducted using JMP Pro 13 (SAS Institute, Inc., Cary, NC). The least squares fit analysis was used to determine the effect of each parameter.

Results

Tumor response

We plotted the VEV vs. the tumor response as given by the mRECIST ($N = 27$), and found that tumors with a higher VEV exhibited a greater response to therapy (Fig. 4a). We binned our groups into responders (PR and CR, $N = 12$) and nonresponders (PD and SD, $N = 15$), and tumors that responded to treatment had a statistically higher VEV compared to the nonresponders, with a mean value of 0.96 ± 0.455 vs. 0.57 ± 0.309, ($p = 0.013$), (Fig. 4b). When the mRECIST categories were converted to numeric values for analysis, there was a positive correlation between tumor response and VEV for all groups (Pearson $r = 0.52$, $p = 0.006$).

Multivariate analysis was conducted to understand the impact of patient characteristics. The continuous variables of VEV, age, number of tumors, tumor length, time to follow-up imaging, and number of prior embolizations were examined for correlation to tumor response. Tumor response was correlated to the VEV ($p = 0.006$) and an increased age ($p = 0.049$), (Fig. 4c). Hepatic segment and gender were

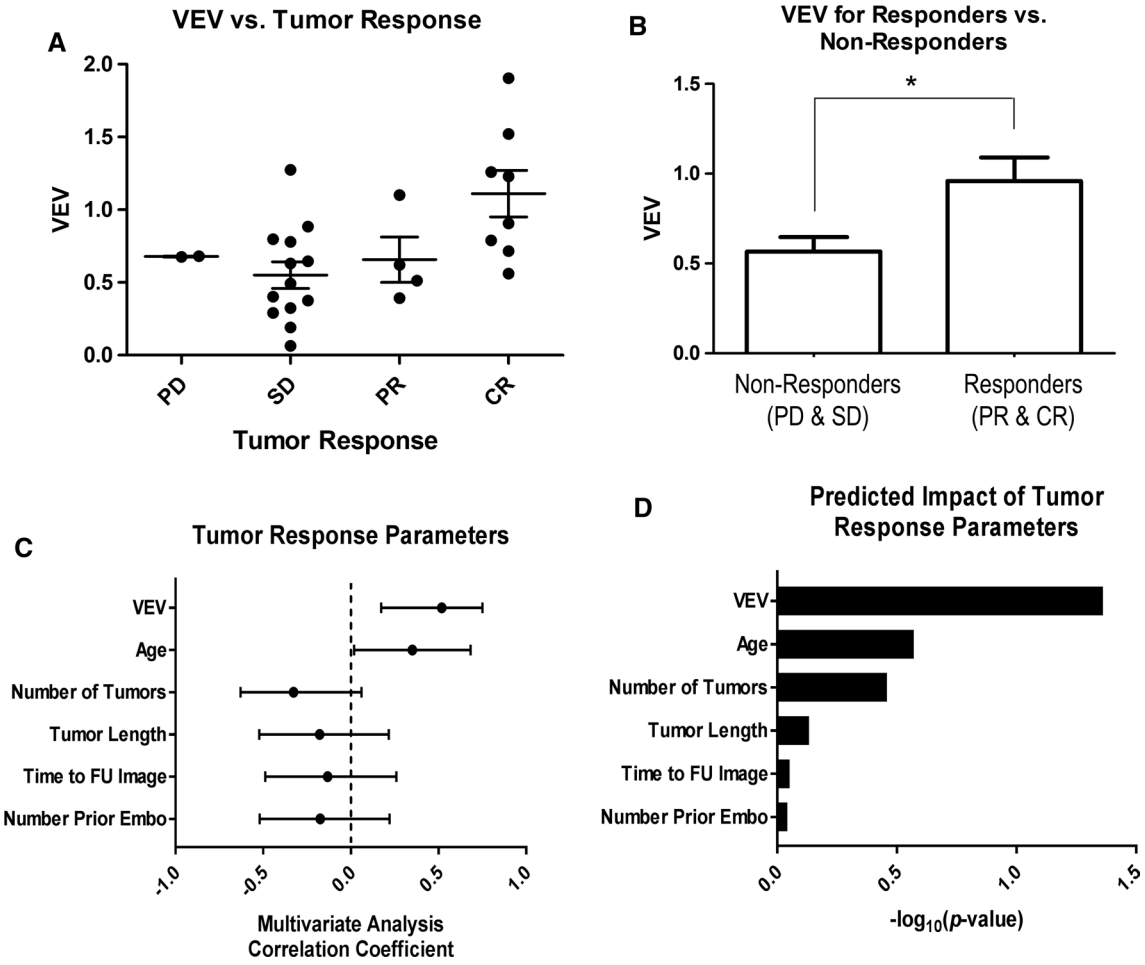

Fig. 4 **a** Algorithm result showing the vascular enhancement value vs. the tumor response by mRECIST. **b** Statistically significant differences between the means of the nonresponders (PD and SD) and the responders (PR and CR), $p = 0.013$. **c** Additional factors of the tumor and treatment were considered using multivariate analysis. Only the VEV ($p = 0.006$) and increased age ($p = 0.049$) showed a significant correlation to the tumor response. Number of tumors ($p = 0.096$), tumor length ($p = 0.372$), time-to-follow-up image ($p = 0.508$), and number of prior embolizations ($p = 0.384$), did not show a statistically significant correlation. **d** Least squares fit regression parameters to estimate the quantitative tumor response to therapy. The VEV was the most heavily weighted when predicting the tumor response ($p = 0.044$), and the only variable in the forward model correlated to the tumor response

examined independently to determine if they influenced the VEV, and neither showed a trend (data not shown). A statistical model of tumor response was created to determine the relative impact of each parameter on the tumor response, and the VEV had the highest probability of predicting the tumor response to therapy ($p = 0.044$), (Fig. 4d).

Discussion

Our study shows that PCA-FI images can be obtained by combining PCA with DSA images obtained during TACE. We utilized procedural images that were readily available to derive the VEV, a parameter that was correlated to tumor response to therapy. Yang et al. [6] demonstrated that increased tumor perfusion resulted in the increased embolic material deposition. Our study was in agreement with this finding as tumors with an increased VEV also exhibited an increased response to therapy.

Other groups have investigated the feasibility of using perfusion CT imaging for early prediction of the response to TACE, supporting the need for a means of early prediction [12–14]. Interestingly, Wimmer et al. found that there was no correlation between pre-TACE perfusion and tumor response which contradicts our findings. We hypothesize that these differences may be due to differences in the imaging method, small sample size, or individual tumor properties. Many of the studies to date have been conducted on limited sample sizes, so additional studies with larger sample sizes are needed to determine the factors driving the observed outcomes. Perfusion CT and DCE-MRI (Dynamic contrast-enhanced MRI) have been investigated to examine tumor perfusion, each with their benefits and limitations for prediction of tumor response [12, 13, 15]. Perfusion CT exposes the patient to increased radiation exposure, and DCE-MRI comes at the expense of imaging acquisition time. We propose that utilizing the procedural angiogram itself may be advantageous in limiting additional radiation exposure and allowing for prediction of tumor response at the time of procedure.

Wang et al. [16] successfully quantitated changes in tumor perfusion using procedural angiograms and DSA; however, their study stopped short of correlating these changes to tumor response. The authors noted several limitations in their study including respiratory motion artifact limiting the application of DSA. Principal component analysis captures the variability in the dataset, which is primarily due to changes in the contrast bolus throughout the time series of images, and therefore minimizes the impact of respiratory motion in the analysis.

We demonstrated that our method was versatile as it was applied to images obtained without modifying the procedural workflow. Calculation of a VEV was possible independent of angiogram length, as the method performed with angiograms with as few as five frames. We hypothesize that even short imaging runs contain significant amounts of predictive data, which in turn limits the radiation exposure to the patient. Another advantage of the method is that it is based on standard numerical analysis techniques. As cone beam CT allows for additional three-dimensional imaging during TACE, our method can be modified to accommodate higher-dimensional datasets.

There are several limitations to this study. We examined parameters that were available in the patient medical record; however, the small sample size may have lowered the significance of any of the parameters in contributing to tumor response. Our study was limited in size since it was an initial proof-of-concept, so a larger sample size that captures additional variables will be useful in determining the predictive capabilities of the VEV.

PCA-FI shows promise as a new method to derive quantitative tumor perfusion data from angiograms, and values derived from PCA-FI can be used to further study tumor vascular characteristics. We demonstrated that the VEV quantitated the tumor blush, and our results suggest that tumor blush is correlated to tumor response to TACE. The VEV may be useful as a point-of-care tool to help select a therapeutic approach or to predict the tumor response to therapy. Future applications of this method may allow for informing the selection of the interventional approach itself.

Funding Jessica Miller was supported by the NIH Medical Scientist Training Program (MSTP) Training Grant: T32 GM007200.

References

1. Mittal S, El-Serag HB (2013) Epidemiology of HCC: Consider the Population. J Clin Gastroenterol 47:S2–6
2. Varela M, Real MI, Burrel M, et al. (2007) Chemoembolization of hepatocellular carcinoma with drug eluting beads: Efficacy and doxorubicin pharmacokinetics. J Hepatol 46(3):474–481
3. Burrel M, Reig M, Forner A, et al. (2012) Survival of patients with hepatocellular carcinoma treated by transarterial chemoembolisation (TACE) using Drug Eluting Beads. Implications for clinical practice and trial design. J Hepatol 56(6):1330–1335
4. Lammer J, Malagari K, Vogl T, et al. (2010) Prospective randomized study of doxorubicin-eluting-bead embolization in the treatment of hepatocellular carcinoma: Results of the PRECISION V study. Cardiovasc Intervent Radiol 33(1):41–52
5. Park HJ, Kin JH, Choi SY, et al. (2017) Prediction of Therapeutic Response of Hepatocellular Carcinoma to Transcatheter Arterial Chemoembolization Based on Pretherapeutic Dynamic CT and Textural Findings. AJR Am J Roentgenol 209(4):W211–W220
6. Yang L, Zhang XM, Zhou XP, et al. (2010) Correlation between tumor perfusion and lipiodol deposition in hepatocellular carcinoma after transarterial chemoembolization. J Vasc Interv Radiol 21(12):1841–1846

7. Wold S, Esbensen K, Geladi P (1987) Principal component analysis. Chemom Intellig Lab Syst 2(1–3):37–52
8. Hillman EM, Moore A (2007) All-optical anatomical co-registration for molecular imaging of small animals using dynamic contrast. Nat Photonics 1(9):526–530
9. Hillman EM, Amoozegar CB, Wang T, et al. (2011) In vivo optical imaging and dynamic contrast methods for biomedical research. Philos Trans A Math Phys Eng Sci 369(1955):4620–4643
10. Miller JP, Wang ST, Orukari I, et al. (2018) Perfusion-based fluorescence imaging method delineates diverse organs and identifies multifocal tumors using generic near-infrared molecular probes. J Biophotonics 11(4):e201700232
11. Lencioni R, Llovet JM (2010) Modified RECIST (mRECIST) assessment for hepatocellular carcinoma. Semin Liver Dis 30(1):52–60
12. Wimmer T, Steiner J, Talakic E, et al. (2017) Computed Tomography Perfusion Following Transarterial Chemoembolization of Hepatocellular Carcinoma: A Feasibility Study in the Early Period. J Comput Assist Tomogr 41(5):708–712
13. Tamandl D, Waneck F, Sieghart W, et al. (2017) Early response evaluation using CT-perfusion one day after transarterial chemoembolization for HCC predicts treatment response and long-term disease control. Eur J Radiol 90:73–80
14. Yang K, Zhang XM, Yang L, et al. (2016) Advanced imaging techniques in the therapeutic response of transarterial chemoembolization for hepatocellular carcinoma. World J Gastroenterol 22(20):4835–4847
15. Taouli B, Johnson RS, Hajdu CH, et al. (2013) Hepatocellular carcinoma: perfusion quantification with dynamic contrast-enhanced MRI. AJR Am J Roentgenol 201(4):795–800
16. Wang J, Cheng JJ, Huang KY, et al. (2016) Quantitative assessment of angiographic perfusion reduction using color-coded digital subtraction angiography during transarterial chemoembolization. Abdom Radiol 41(3):545–552